Electronic Supplementary Material (ESI) for ChemComm.

Supporting Information

Tailoring pore geometry and chemistry in microporous metal–organic frameworks for high methane storage working capacity

Kai Shao,[a] Jiyan Pei,[a] Jia-Xin Wang,[a] Yu Yang,[a] Yuanjing Cui,[a] Wei Zhou,[b] Taner Yildirim,[b] Bin Li,*[,a] Banglin Chen,[c] Guodong Qian*[,a]

[a] State Key Laboratory of Silicon Materials, Cyrus Tang Center for Sensor Materials and Applications, Department of Materials Science & Engineering, Zhejiang University, Hangzhou 310027, China. E-mail: bin.li@zju.edu.cn; gdqian@zju.edu.cn

[b] NIST Center for Neutron Research, National Institute of Standards and Technology, Gaithersburg, Maryland 20899-6102, United States

[c] Department of Chemistry, University of Texas at San Antonio, One UTSA Circle, San Antonio, Texas 78249-0698, USA. Fax: (+1)-210-458-7428

1. Materials and General Methods

All the chemicals were commercially available and used without further purification. ^{1}H NMR spectra were recorded on a Bruker Advance DMX500 spectrometer using tetramethylsilane(TMS) as an internal standard. Elemental analyses for C, H, and N were performed on an EA1112 microelemental analyzer. Powder X-ray diffraction (PXRD) patterns were collected in the 2θ=3-45^o range on an X'Pert PRO diffractometer with Cu K_α radiation (λ=1.542Å) at room temperature. Thermogravimetric analyses (TGA) were conducted on a Netszch TGA 209 F3 thermogravimeter with a heating rate of 5 ^{o}C min^{-1} in a N_2 atmosphere.

2. Gas sorption Measurements

A Micromeritics ASAP 2020 surface area analyzer was used to measure gas adsorption isotherms. To remove all the guest solvents in the framework, the fresh samples of ZJU-105 and PCN-46 were guest-exchanged with dry acetone at least 10 times, filtered and degassed at room temperature for 1 day and then at 373 K for another 9 h until the minimal pressure before the measurements were made. The activated samples of ZJU-105 and PCN-46 were maintained at 77 K with liquid nitrogen. High-pressure CH_4 sorption isotherms were measured using a Sieverts-type apparatus. A detailed description of the experimental setup, calibration and the isotherm has been published previously.[1]

3. X-ray Crystallography

The crystal data were collected on an Agilent Supernova CCD diffractometer equipped with a graphite-monochromatic enhanced Cu Kα radiation (λ = 1.54184 Å) at 296 K. The datasets were corrected by empirical absorption correction using spherical harmonics, implemented in the SCALE3 ABSPACK scaling algorithm. The structure was solved by direct methods using SIR92 and refined by full matrix least-squares methods with the SHELX-2014 program package. The solvent molecules in the compound are highly disordered. The SQUEEZE subroutine of the PLATON software suite was used to remove the scattering from the highly disordered guest molecules.[2] The resulting new files were used to further refine the structures. The H atoms on C atoms were generated geometrically. Crystal data are summarized in Table S1.

4. Derivation of the isosteric heat of adsorption (Q_{st})

A virial type expression of the following form was used to fit the CH_4 total adsorption isotherm data at 273 K and 298 K.

$$\ln P = \ln N + 1/T \sum_{i=0}^{m} a_i N^i + \sum_{i=0}^{n} b_i N^i$$

Here, P is the pressure expressed in bar, N is the amount adsorbed in cc(STP)/cc, T is the temperature in K, a_i and b_i are virial coefficients, and m, n represents the number of coefficients required to adequately describe the isotherms. m and n were gradually increased until the contribution of extra added a and b coefficients was deemed to be statistically insignificant towards the overall fit, as determined using the average value of the squared deviations from the experimental values was minimized. The values of the virial coefficients a_0 through a_m were then used to calculate the isosteric heat of adsorption using the following expression.

$$Q_{st} = -R \sum_{i=0}^{m} a_i N^i$$

Here, Q_{st} is the coverage-dependent isosteric heat of adsorption and R is the universal gas constant of 8.3147 J $K^{-1}mol^{-1}$.

Scheme S1. Synthetic routes to the organic linker H_4L1

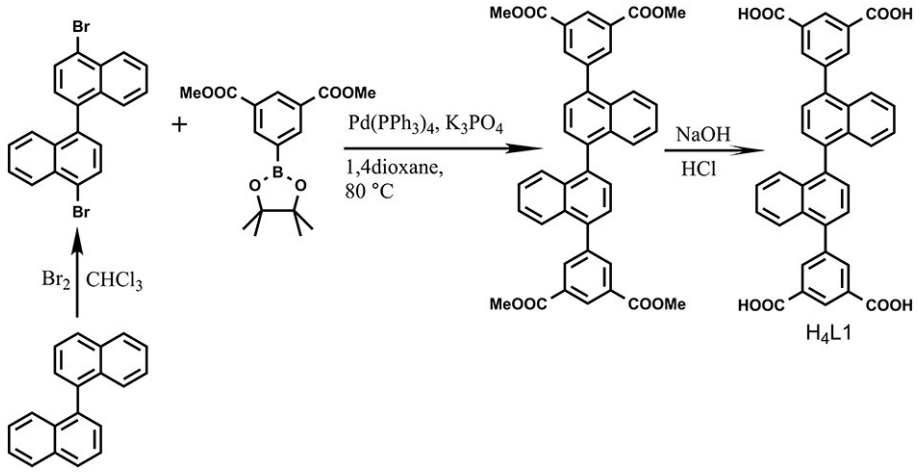

4,4'-dibromo-1,1'-binaphthalene: 1,1'-binaphthalene (0.79 g, 3.1 mmol) was dissolved in chloroform (30 mL) and the solution was cooled to 0 °C with an ice-bath. To the solution was added bromine (2.6 g, 16 mmol) over 20 min. After the mixture stirred for 2.5 h, aqueous sodium sulfite was added for quenching. The organic layer was separated and washed with brine, dried over anhydrous sodium sulfate. After filtration, the filtrate was evaporated and the residue was recrystallized from chloroform to give white crystals (0.80 g, 61%). ^{1}H NMR (500 MHz, Chloroform-d) δ 8.36 (d, J = 8.5 Hz, 2H), 7.90 (d, J = 7.5 Hz, 2H), 7.60 (td, J_1 = 8.4 Hz, J_2 = 4.0 Hz, 2H), 7.36–7.31 (m, 6H).

Tetramethyl 5,5'-([1,1'-binaphthalene]-4,4'-diyl)diisophthalate: 4,4'-dibromo-1,1'-binaphthalene (0.82 g, 2 mmol), 5-(4,4,5,5-tetramethyl-1,3,2-dioxaborolan-2-yl) isophthalate (2.03 g, 6 mmol), K_3PO_4 (2.55g, 12 mmol) and tetrakis(triphenylphosphine) palladium(0) (0.1 g, 0.09 mmol) were dissolved in dry 1,4-dioxane (60 mL) under N_2 atmosphere. The mixture was stirred at 80 ^{o}C for three days. After removal of organic solvent under vacuum, the residue was washed with water and extracted with dichloromethane. The organic layer was dried with anhydrous $MgSO_4$ and the solvent was removed under vacuum. The crude product was purified by column chromatography (silica gel, dichloromethane /petroleum ether, 3:1 v/v). Yield: 67% (0.85 g). ^{1}H NMR (500 MHz, Chloroform-d) δ 8.82 (t, J = 1.6 Hz, 2H), 8.50 (d, J = 1.7 Hz, 4H), 7.87 (d, J = 8.4 Hz, 2H), 7.62 (d, J = 7.1 Hz, 2H), 7.58 (d, J = 7.1 Hz, 2H), 7.57–7.54 (m, 2H), 7.48 (td, J_1 = 8.4 Hz, J_2 = 1.3 Hz, 2H), 7.37 (td, J_1 = 8.2 Hz, J_2 = 1.2 Hz, 2H), 4.00 (s, 12H).

5,5'-([1,1'-binaphthalene]-4,4'-diyl)diisophthalic acid (H_4L1): tetramethyl 5,5'-([1,1'-binaphthalene]-4,4'-diyl)diisophthalate (0.85 g, 1.3 mmol) was suspended in 50 mL THF, and then a 2M KOH aqueous solution (50 mL) was added. The mixture was stirred under reflux overnight until it became clear. After that THF was removed under reduced pressure and dilute HCl was then added to the remaining aqueous solution to acidify pH = 2. The precipitate was collected by filtration, washed with water for several times, and dried to afford white powder. Yield: 736 mg (95%). ^{1}H NMR (500 MHz, DMSO-d6) δ 13.46 (s, 4H), 8.62 (d, J = 1.7 Hz, 2H), 8.35 (d, J = 1.6 Hz, 4H), 7.87 (d, J = 8.6 Hz, 2H), 7.71 (d, J = 7.2 Hz, 2H), 7.68 (d, J = 7.2 Hz, 2H), 7.57 (td, J_1 = 8.3 Hz, J_1 = 2.2 Hz, 2H), 7.47–7.42 (m, 4H).

Scheme S2. Synthetic routes to the organic linker H_4L2

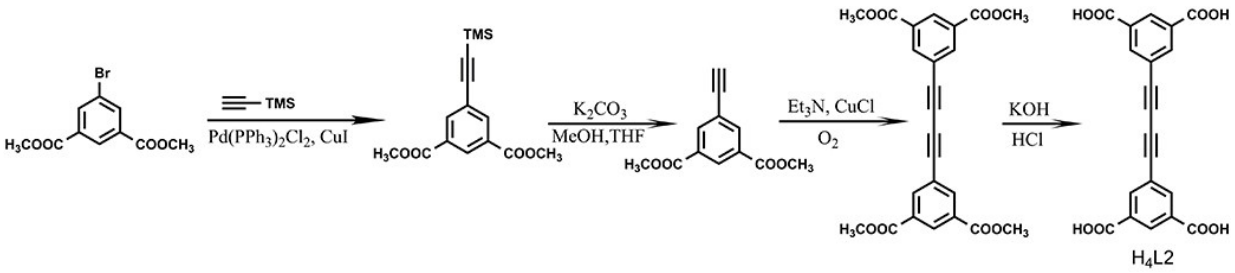

Dimethyl 5-(2-(trimethylsilyl)ethynyl)isophthalate: Dimethyl 5-bromoisophthalate (10.00 g, 36.62 mmol), CuI (0.35 g, 1.83 mmol), and $Pd(PPh_3)_2Cl_2$ (1.28 g, 1.83 mmol) were placed in a 500 mL round-bottom flask. The flask was evacuated under vacuum and refilled with N_2 for three times, and then ethynyltrimethylsilane (7.6 mL, 54.93 mmol), dry THF (200 mL) and triethylamine (7.7 mL, 54.93 mmol) were added via syringe sequentially. The resulting solution was stirred under nitrogen at room temperature for 24 h. After removal of the volatile, CH_2Cl_2 (100 mL) and H_2O (100 mL) was added. The organic phase was separated, and the aqueous phase was extracted with CH_2Cl_2. The organic phase was combined, washed with brine, dried over anhydrous $MgSO_4$ and filtered. The solvent was removed under vacuum, and the residue was purified using silica gel column chromatography with petroleum ether/ethyl acetate (30/1, v/v) as eluent, affording dimethyl 5-(2-(trimethylsilyl)ethynyl)isophthalate as a yellow solid in 87 % yield (9.2 g). ^{1}H NMR (500 MHz, Chloroform-d) δ 8.60 (t, J = 1.6 Hz, 1H), 8.29 (d, J = 1.7 Hz, 2H), 3.95 (s, 6H), 0.26 (s, 9H).

Dimethyl 5-ethynylisophthalate: A mixture of dimethyl 5-(2-(trimethylsilyl)ethynyl)isophthalate (9.2 g, 31.68 mmol), K_2CO_3 (0.88 g, 6.30 mmol) in a mixed solvent of THF (70 mL) and MeOH (175 mL) was stirred under a nitrogen atmosphere at room temperature for 24 h. After that, the solvent was removed under vacuum. CH_2Cl_2 (100 mL) and H_2O (100 mL) were added. The organic phase was separated, and the aqueous phase was extracted with CH_2Cl_2. The organic phase was combined, washed with brine, dried over anhydrous $MgSO_4$ and filtered. The removal of volatile gave dimethyl 5-ethynylisophthalate in 94 % yield (6.5 g), which is pure enough for the next reactions. ^{1}H NMR (500 MHz, Chloroform-d) δ 8.63 (t, *J* = 1.6 Hz, 1H), 8.32 (d, *J* = 1.7 Hz, 2H), 3.95 (s, 6H), 3.17 (s, 1H).

Tetramethyl 5,5'-(buta-1,3-diyne-1,4-diyl)diisophthalate: Anhydrous Et_3N (20 ml) and tetrahydrofuran (20 mL) were added to a flask containing a mixture of dimethyl 5-ethynylisophthalate (4.2 g, 19 mmol), $Pd(PPh_3)_2Cl_2$ (0.27 g, 0.38 mmol) and cuprous chloride (0.08 g, 0.77 mmol). The resulting mixture was heated at 50 ^{o}C for 24 h during which oxygen was bubbled into the solution. The solvent was removed in vacuo and the residue was extracted with dichloromethane and saturated ammonium chloride solution, and dried over anhydrous $MgSO_4$. After filtration and evaporation, flash column chromatography on silica gel using dichloromethane as eluant gave the product. Yield: 3 g (36 %). ^{1}H NMR (500 MHz, Chloroform-d) δ 8.66 (t, *J* = 1.6 Hz, 2H), 8.36 (d, *J* = 1.6 Hz, 4H), 3.96 (s, 12H).

5,5'-(buta-1,3-diyne-1,4-diyl)diisophthalic acid (H_4L2): To a stirred solution of tetramethyl 5,5'-(buta-1,3-diyne-1,4-diyl)diisophthalate (2 g) in methanol/water (V :V = 9 : 1, 60 mL), potassium hydroxide (4.2 g) was added and the mixture was heated at 80 ^{o}C for 24 h, then acidified with 6M hydrochloric acid. The precipitate was removed by filtration, washed with water for several times, and dried in vacuo. Yield 1.45 g (83 %). ^{1}H NMR (500 MHz, DMSO-d6) δ 13.57 (s, 4H), 8.49 (t, *J* = 1.7 Hz, 2H), 8.29 (d, *J* = 1.6 Hz, 4H).

Synthesis of ZJU-105

A mixture of the organic linker H_4L1 (10 mg, 0.017 mmol) and $Cu(NO_3)_2 \cdot 2.5H_2O$ (25 mg, 0.107 mmol) was dissolved into a mixed solvent (DMF/H_2O, 3 mL/0.2 mL) in a screw-capped vial (20 mL), to which 20 μL of 37% HCl was added. The vial was capped and heated in an oven at 80 ^oC for 72 h. Blue block crystals were obtained by filtrated and washed with DMF several times to afford ZJU-105 in 70% yield. ZJU-105 has a best formula as $[Cu_2L1(H_2O)_2] \cdot 5DMF \cdot 3H_2O$, which was obtained based on single-crystal X-ray structure determination, elemental analysis and TGA. Anal. Calcd for $C_{51}H_{59}N_5O_{18}Cu_2$: C, 51.30; H, 4.95; N, 5.87; found: C, 51.43; H, 4.91; N, 5.81. TGA data for loss of 5 DMF and $5H_2O$: calcd: 38.18 %, found: 38.46 %.

Synthesis of PCN-46

A mixture of the organic linker H_4L2 (10 mg, 0.026 mmol) and $Cu(NO_3)_2 \cdot 2.5H_2O$ (20 mg, 0.086 mmol) was dissolved into a mixed solvent (DMF/EtOH/H_2O, 2.4 mL/1 mL/1 mL) in a screw-capped vial (20 mL), to which 70 μL HNO_3 was added. The vial was capped and heated in an oven at 85 ^oC for 24 h. Green block crystals were obtained by filtrated and washed with DMF several times to afford PCN-46 in 68% yield. PCN-46 has a best formula as $[Cu_2L2(H_2O)_2] \cdot 4DMF \cdot 5H_2O$, which was obtained based on single-crystal X-ray structure determination, elemental analysis and TGA. Anal. Calcd for $C_{32}H_{56}N_4O_{19}Cu_2$: C, 41.75; H, 6.09; N, 6.09; found: C, 41.71; H, 6.12; N, 6.14. TGA data for loss of 4DMF and $7H_2O$: calcd: 44 %, found: 44.3 %.

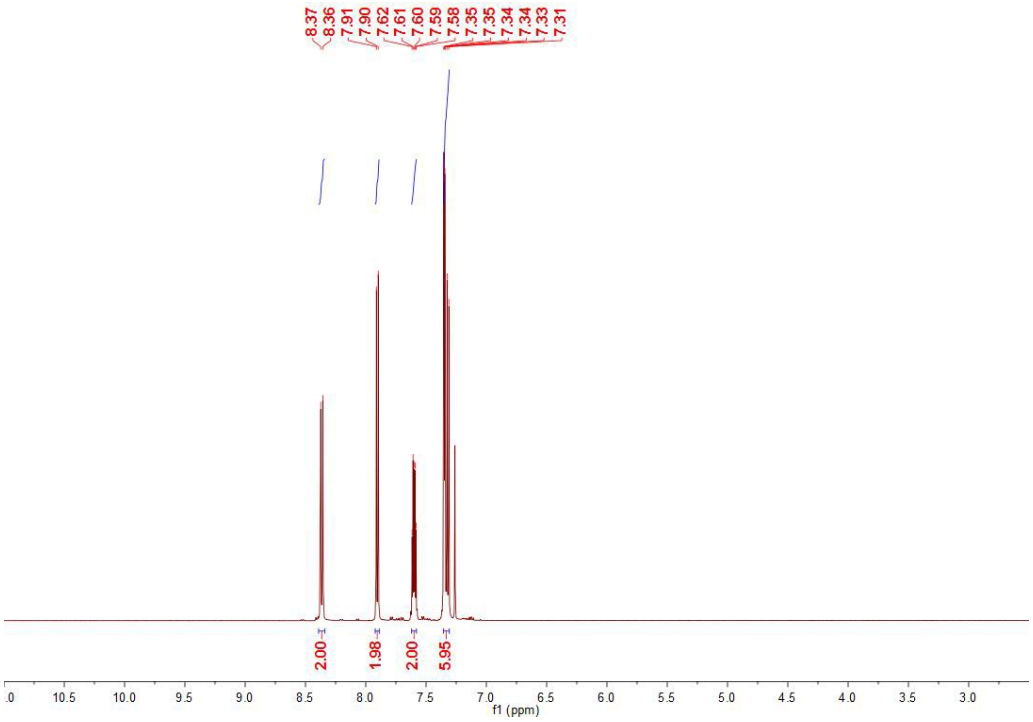

Figure S1. ^{1}H ($CDCl_3$, 500MHz) spectra of 4,4'-dibromo-1,1'-binaphthalene.

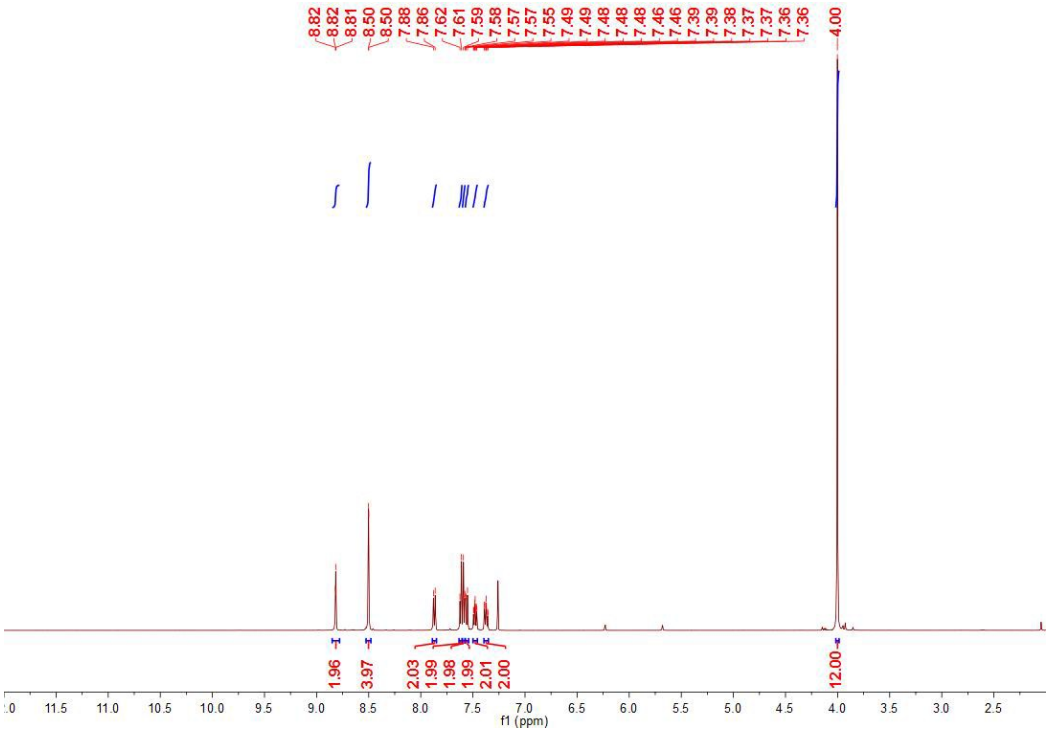

Figure S2. ^{1}H ($CDCl_3$, 500MHz) spectra of Tetramethyl 5,5'-([1,1'-binaphthalene]-4,4'-diyl)diisophthalate.

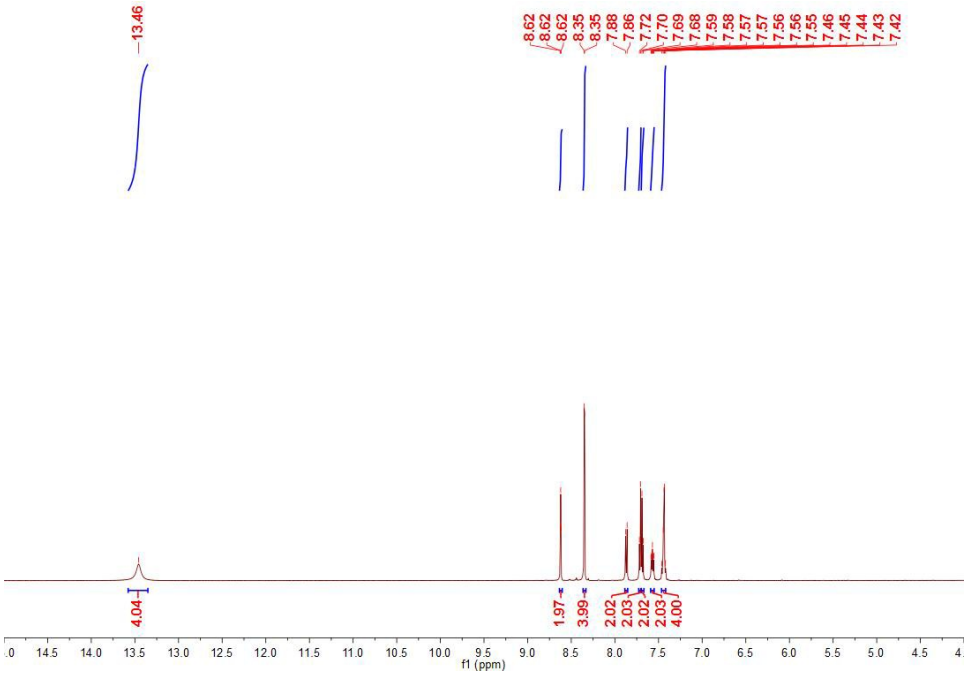

Figure S3. ^{1}H (DMSO, 500MHz) spectra of 5,5'-([1,1'-binaphthalene]-4,4'-diyl)diisophthalic acid.

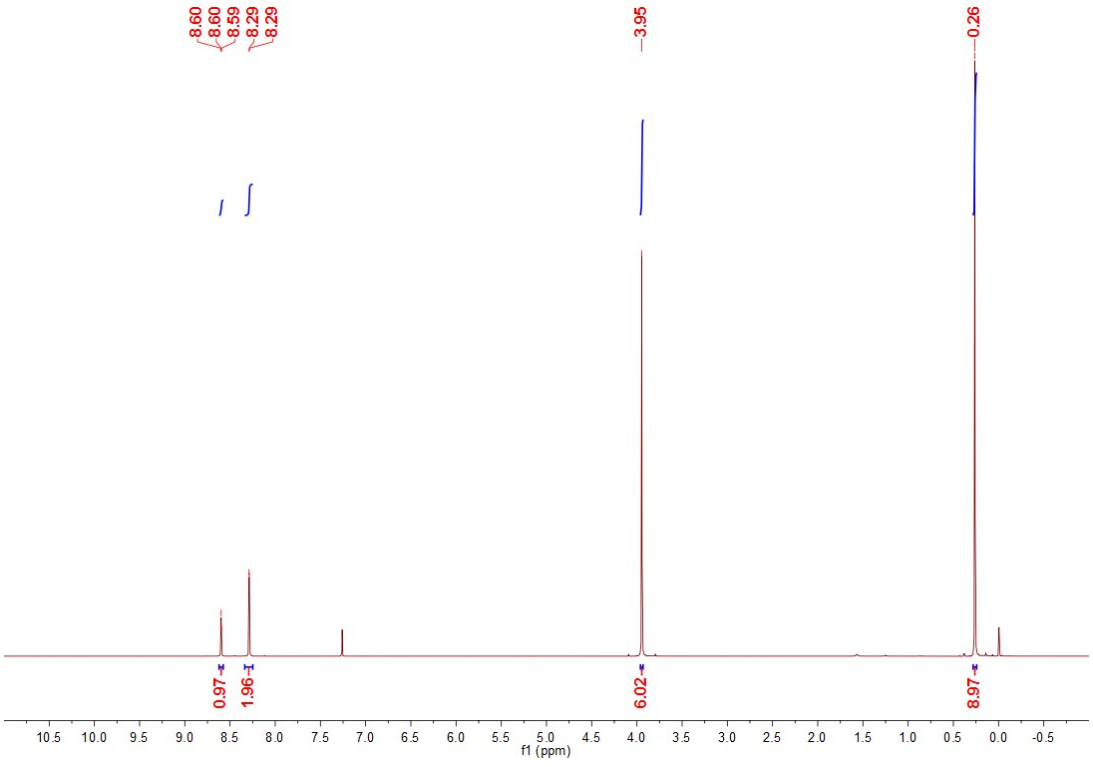

Figure S4. ^{1}H ($CDCl_3$, 500MHz) spectra of Dimethyl 5-(2-(trimethylsilyl)ethynyl)isophthalate.

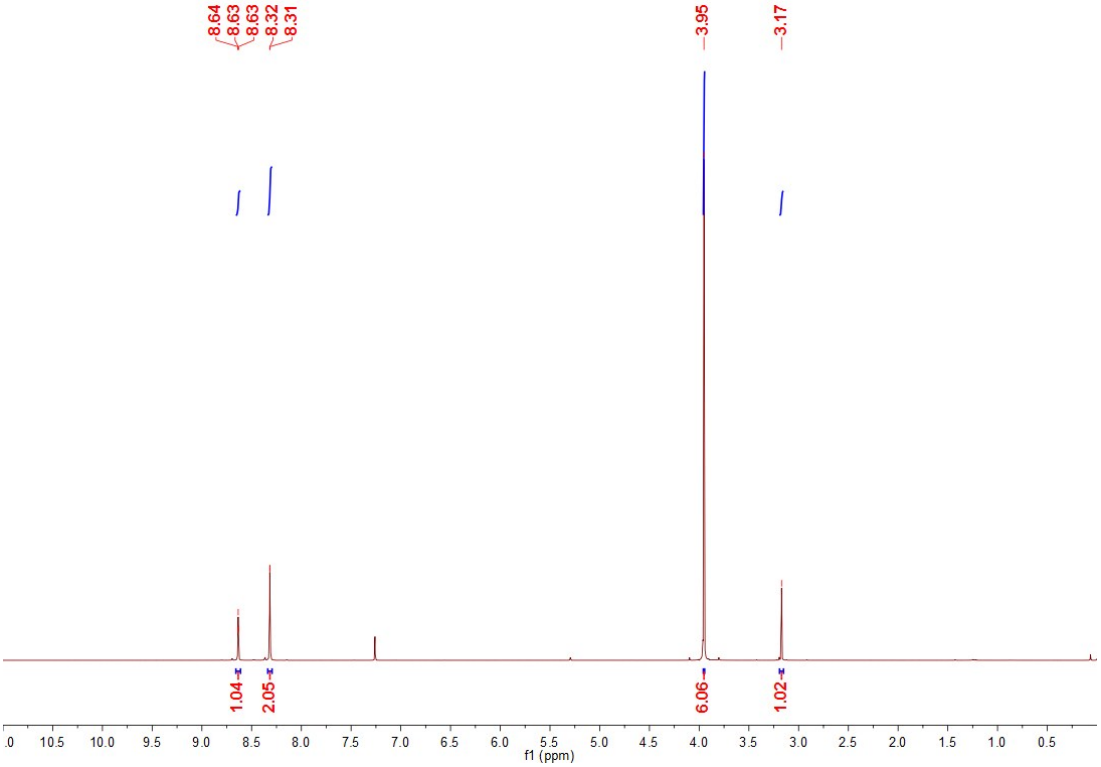

Figure S5. ^{1}H ($CDCl_3$, 500MHz) spectra of Dimethyl 5-ethynylisophthalate.

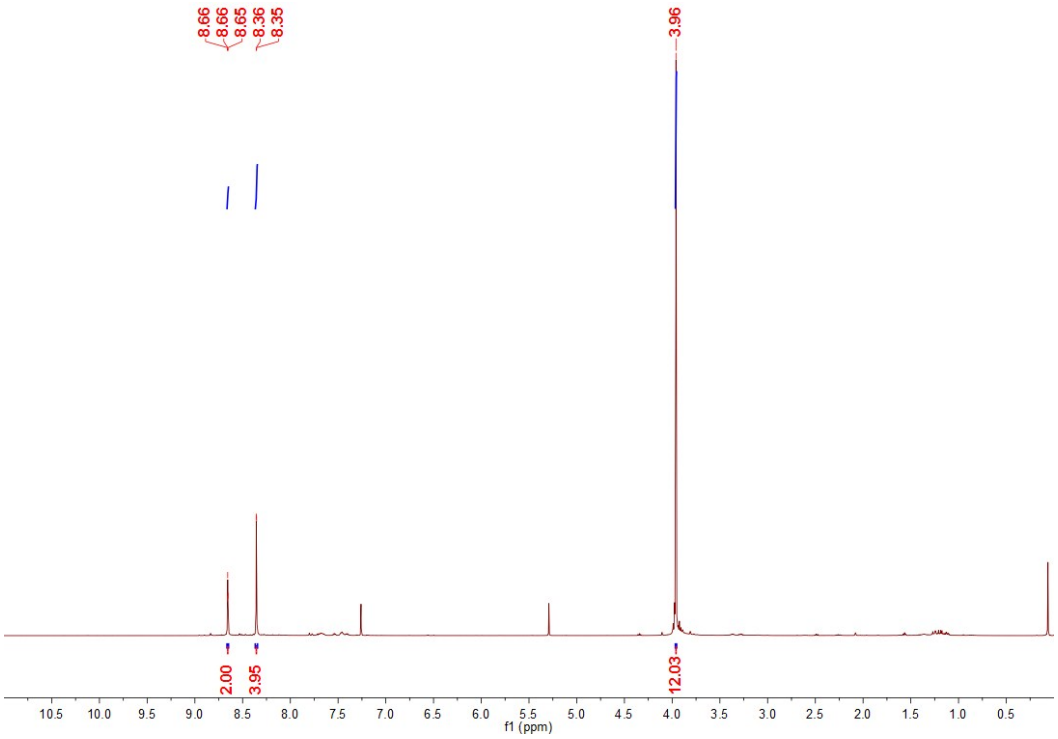

Figure S6. ^{1}H ($CDCl_3$, 500MHz) spectra of Tetramethyl 5,5'-(buta-1,3-diyne-1,4-diyl)diisophthalate.

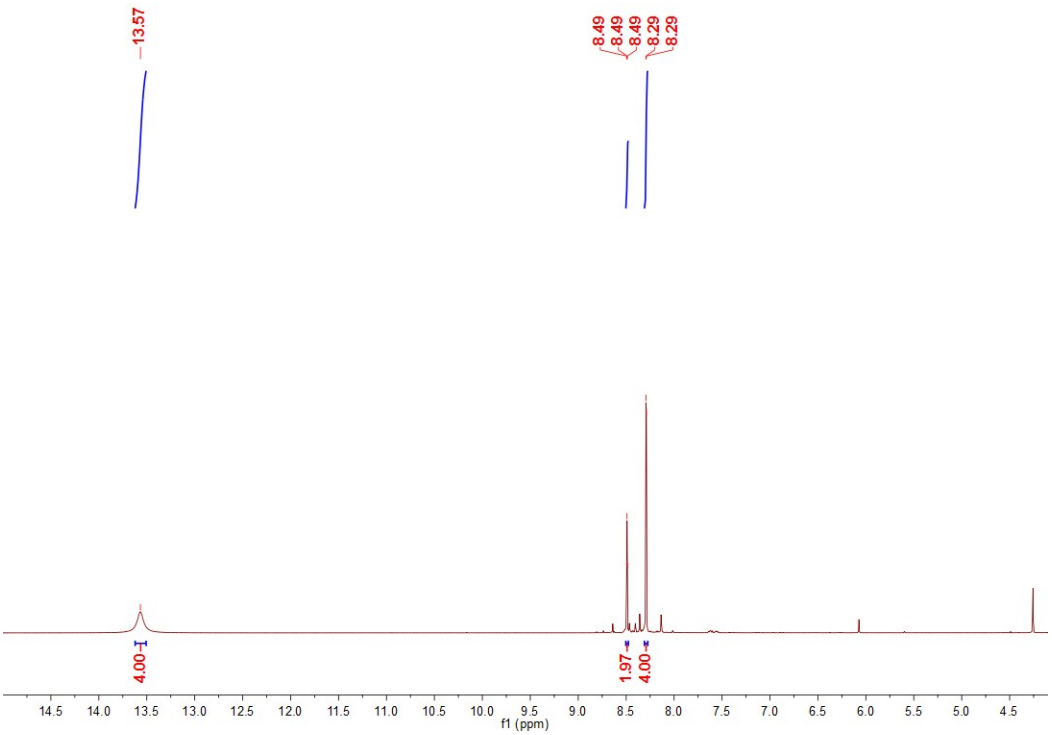

Figure S7. ^{1}H (DMSO, 500MHz) spectra of 5,5'-(buta-1,3-diyne-1,4-diyl)diisophthalic acid

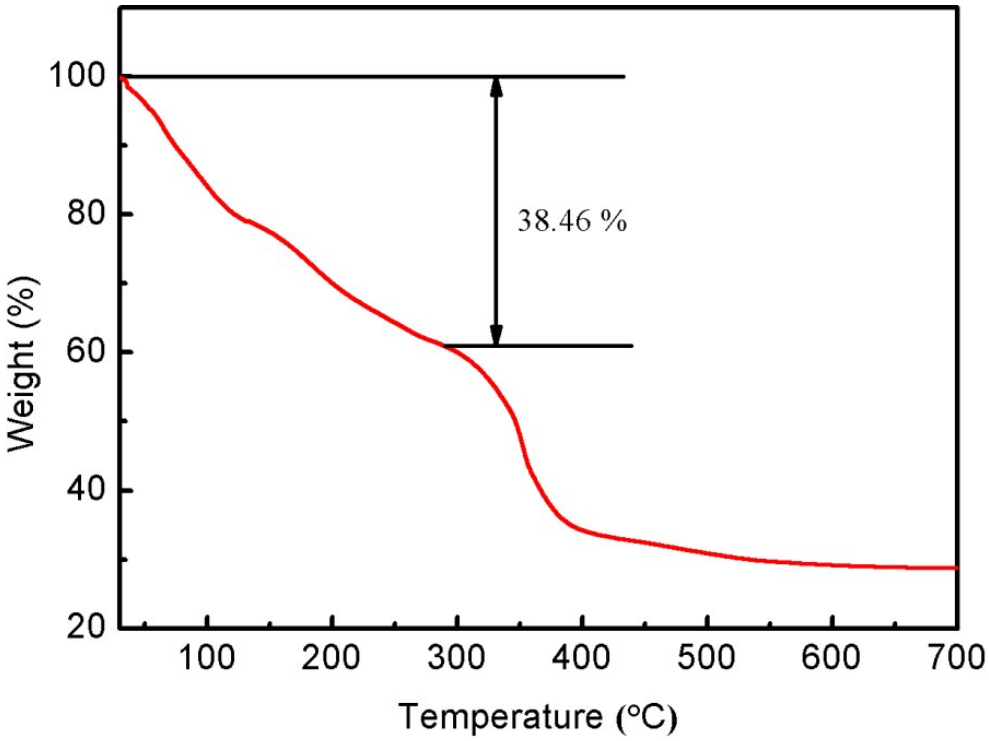

Figure S8. TGA curves of as-synthesized ZJU-105.

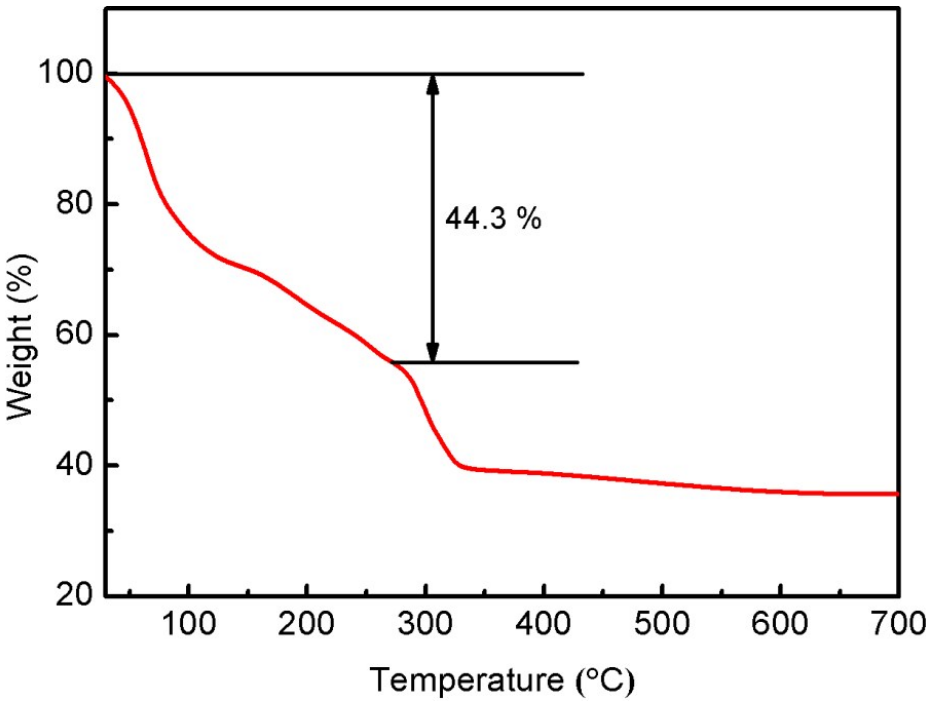

Figure S9. TGA curves of as-synthesized PCN-46.

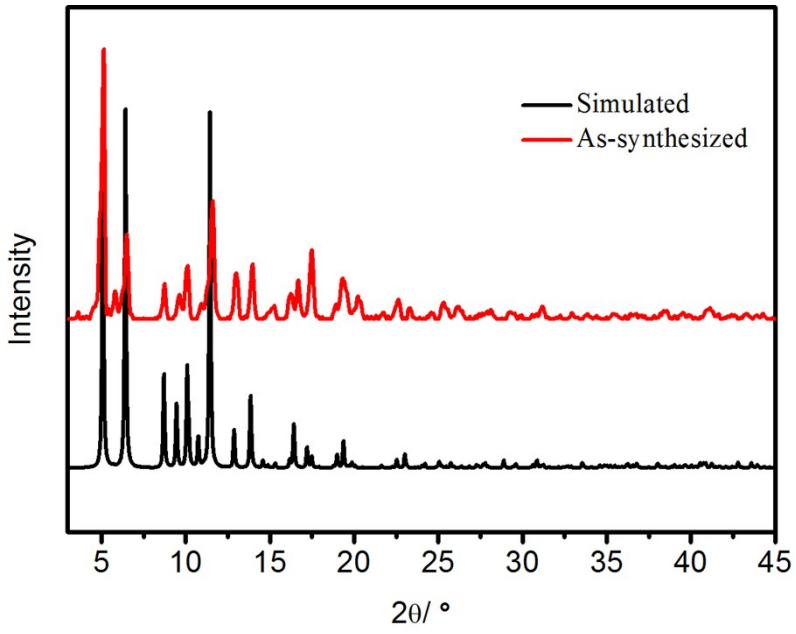

Figure S10. PXRD patterns of as-synthesized ZJU-105 (red) along with the simulated XRD pattern from the single-crystal X-ray structure (black).

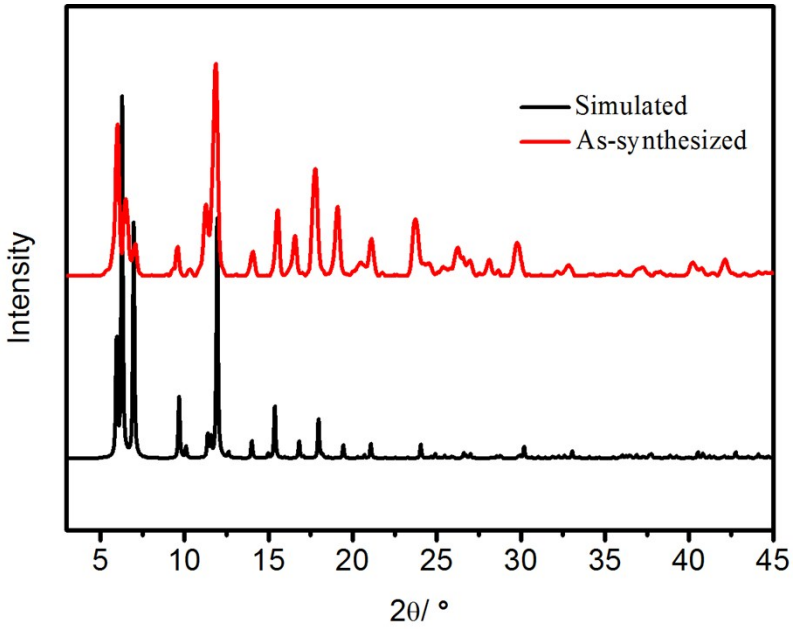

Figure S11. PXRD patterns of as-synthesized PCN-46 (red) along with the simulated XRD pattern from the single-crystal X-ray structure (black).

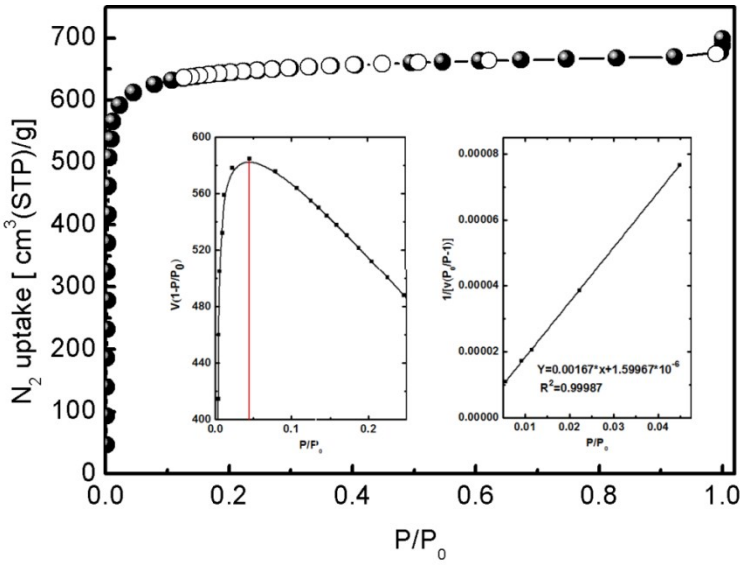

Experimental values:

S_{BET} = (1/(0.00167- 1.59967×10^{-6}))/22414 ×6.02×10^{23}×0.162×10^{-18}= 2608 m^2 g^{-1}

V_P = 1.037 cm^3/g

Theoretical values calculated from the crystal structure:

S_{BET} = 2452 m^2 g^{-1}; V_P = 0.96 cm^3/g

Figure S12. N_2 sorption isotherms of ZJU-105a at 77 K. Solid symbols: adsorption, open symbols: desorption.

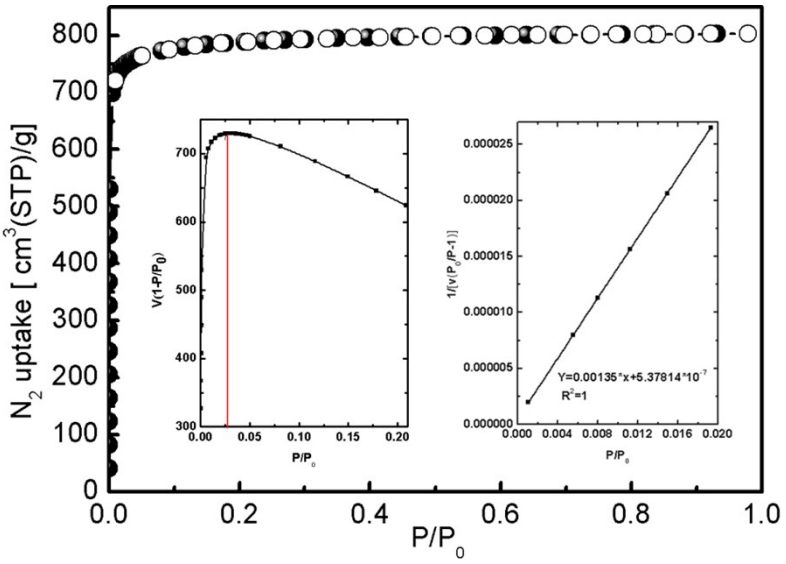

Experimental values:

S_{BET} = (1/(0.00135- 5.37814×10^{-7}))/22414 ×6.02×10^{23}×0.162×10^{-18}= 3224 m^2 g^{-1}

V_P = 1.243 cm^3/g

Theoretical values calculated from the crystal structure:

S_{BET} = 3634 m^2 g^{-1}; V_P = 1.266 cm^3/g

Figure S13. N_2 sorption isotherms of PCN-46a at 77 K. Solid symbols: adsorption, open symbols: desorption.

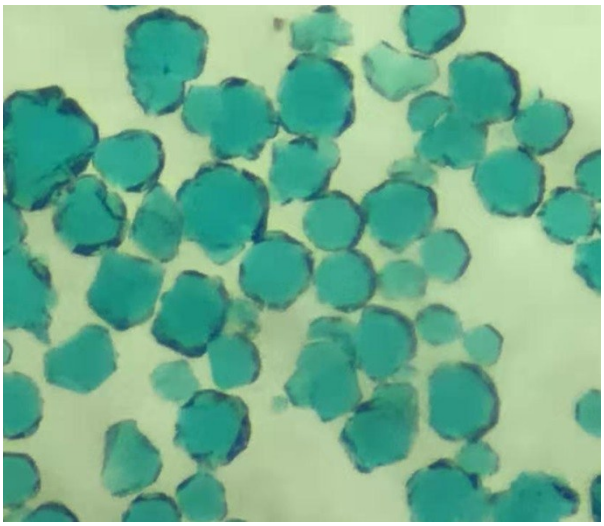

Figure S14. Optical images of the as-synthesized crystals of ZJU-105.

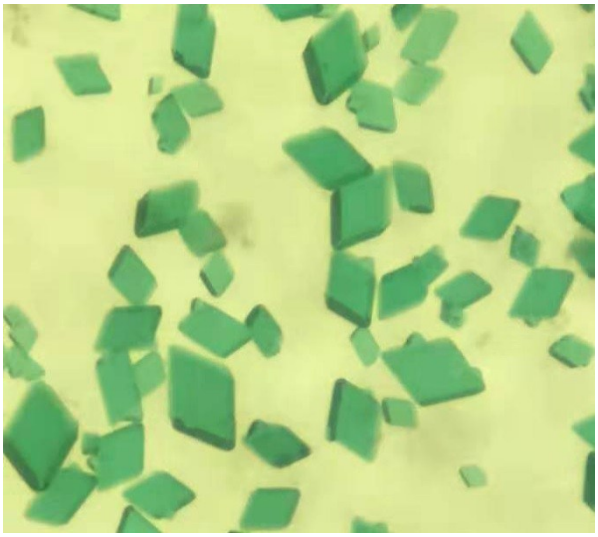

Figure S15. Optical images of the as-synthesized crystals of PCN-46.

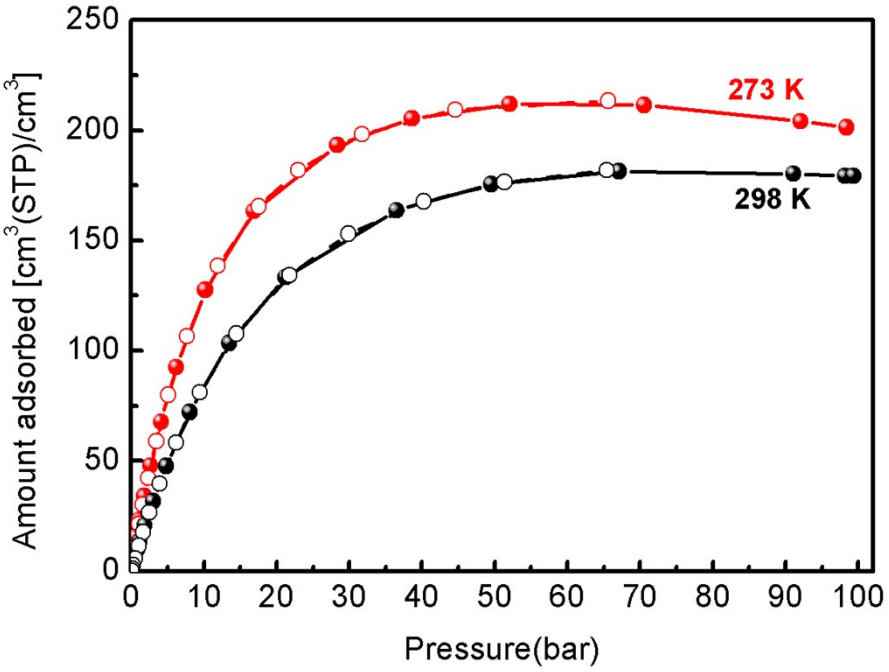

Figure S16. Excess volumetric high-pressure methane sorption isotherms of ZJU-105a at different temperatures. Filled and open symbols represent adsorption and desorption data, respectively.

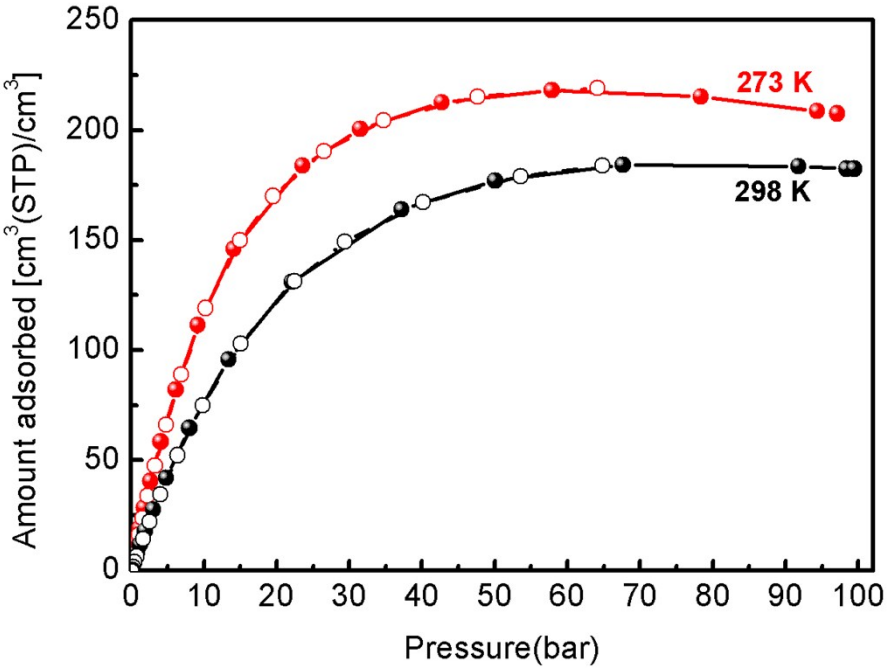

Figure S17. Excess volumetric high-pressure methane sorption isotherms of PCN-46a at different temperatures. Filled and open symbols represent adsorption and desorption data, respectively.

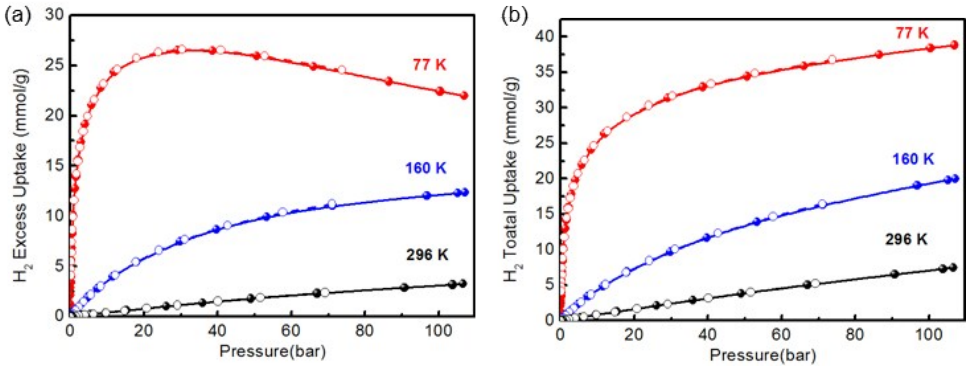

Figure S18. Excess (a) and total (b) high-pressure H_2 sorption isotherms of ZJU-105a at different temperatures. Filled and open symbols represent adsorption and desorption data, respectively.

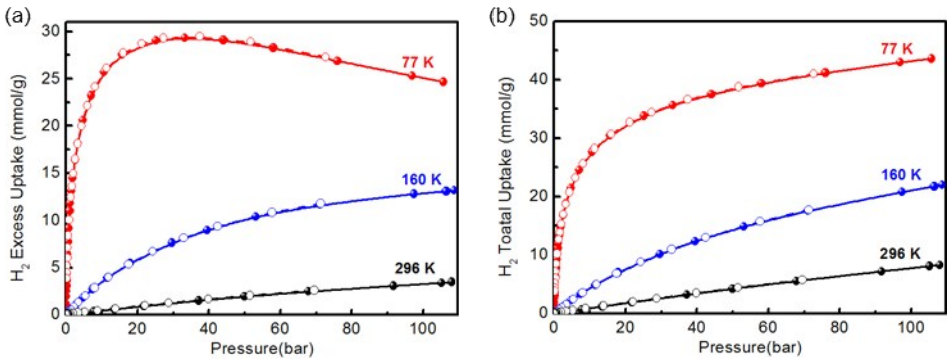

Figure S19. Excess (a) and total (b) high-pressure H_2 sorption isotherms of PCN-46a at different temperatures. Filled and open symbols represent adsorption and desorption data, respectively.

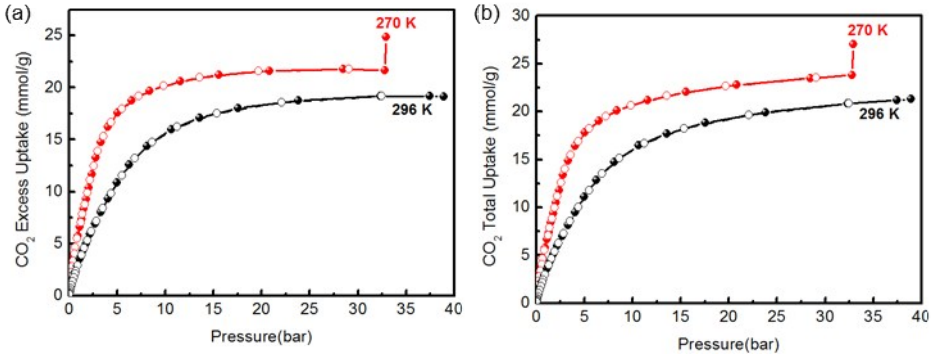

Figure S20. Excess (a) and total (b) high-pressure CO_2 sorption isotherms of ZJU-105a at different temperatures. Filled and open symbols represent adsorption and desorption data, respectively.

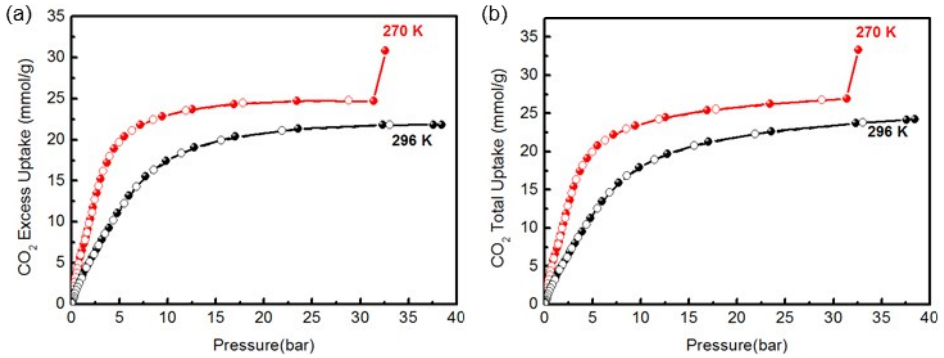

Figure S21. Excess (a) and total (b) high-pressure CO_2 sorption isotherms of PCN-46a at different temperatures. Filled and open symbols represent adsorption and desorption data, respectively.

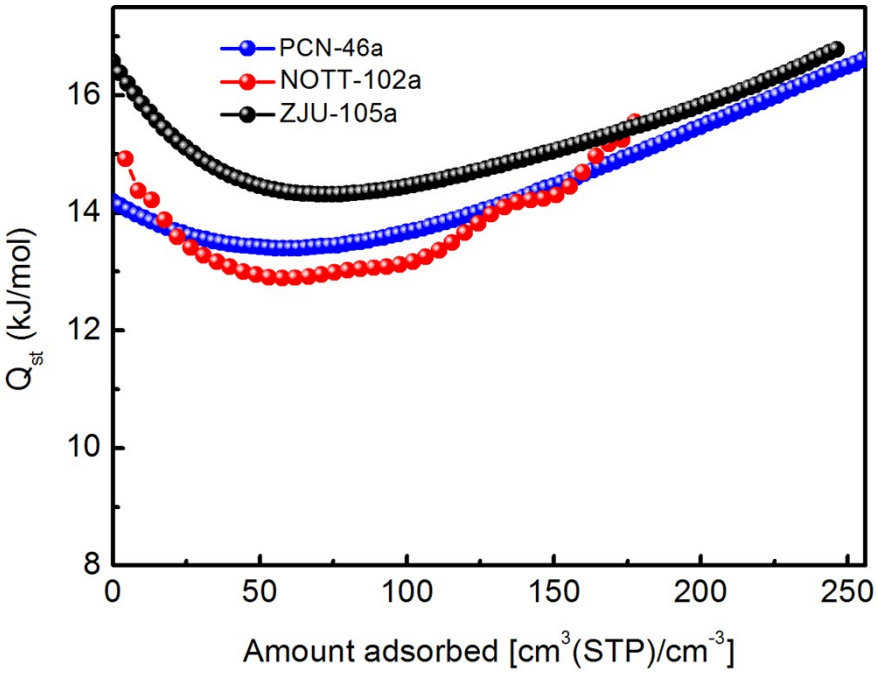

Figure S22. Comparison of Q_{st} for CH_4 adsorption for ZJU-105a, NOTT-102a, and PCN-46a.

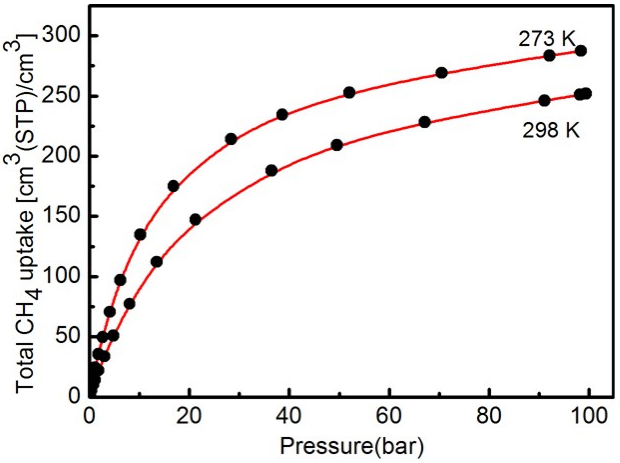

a_i	b_i
-1993.8277	4.14653
9.7484	-0.02643
-0.12121	3.57125E-4
6.44987E-4	-1.80878E-6
-1.69038E-6	4.8168E-9
1.66651E-9	-4.61235E-12

Figure S23. Derivation of Q_{st} for CH_4 adsorption in ZJU-105a from virial fitting of the total adsorption isotherm data. The virial coefficients are shown on the right.

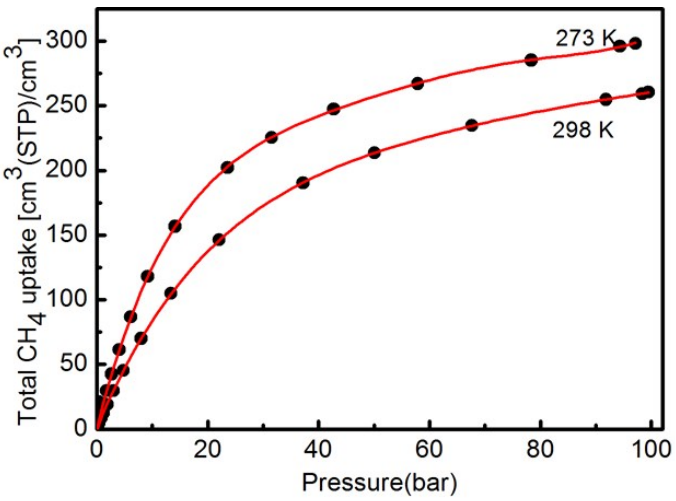

a_i	b_i
-1709.16333	3.38125
3.69663	-0.00821
-0.04054	1.1241E-4
1.09031E-4	-2.15465E-7
-6.36331E-8	2.20888E-11
-1.21485E-10	5.5589E-13

Figure S24. Derivation of Q_{st} for CH_4 adsorption in PCN-46a from virial fitting of the total adsorption isotherm data. The virial coefficients are shown on the right.

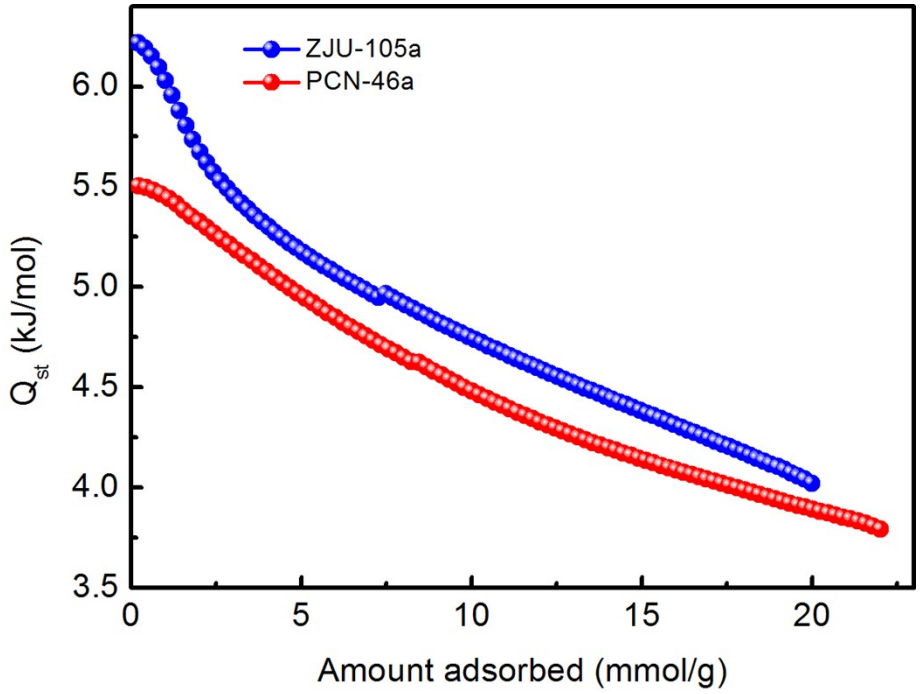

Figure S25. Comparison of Q_{st} for H_2 adsorption for ZJU-105a and PCN-46a.

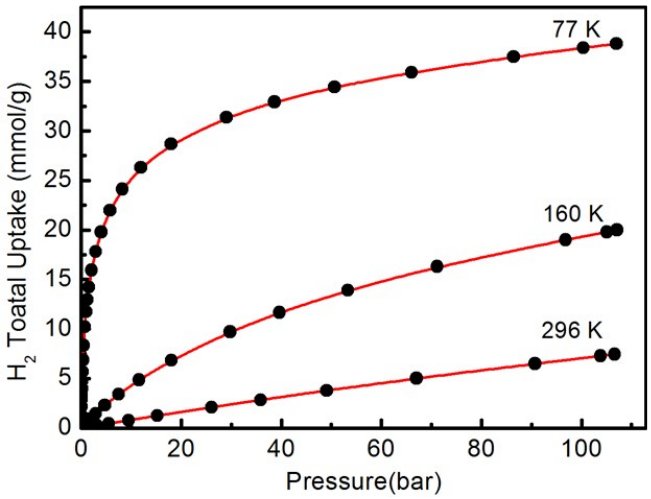

a_i	b_i
-759.53	5.1809
40.874	-0.16657
-3.3714	0.017668
0.13843	-0.00059834
-0.0014485	-6.0169E-6
-2.2621E-5	4.8828E-7

Figure S26. Derivation of Q_{st} for H_2 adsorption in ZJU-105a from virial fitting of the total adsorption isotherm data. The virial coefficients are shown on the right.

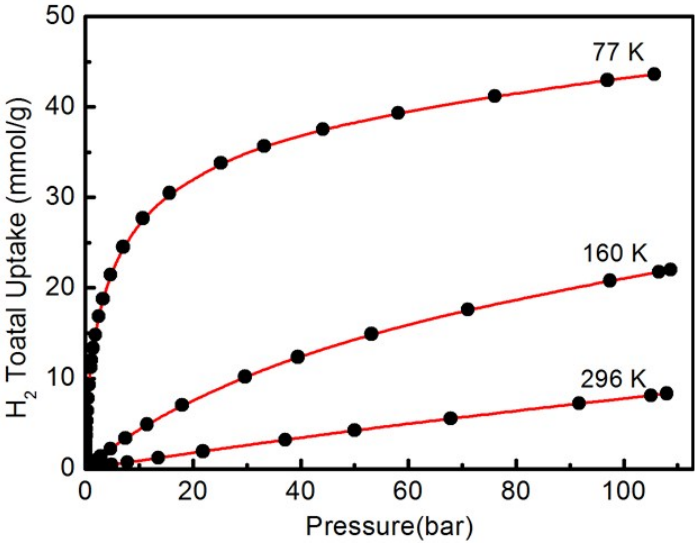

a_i	b_i
-664.87	4.7092
13.843	-0.045874
-0.024747	0.0029031
-0.01231	-0.00021047
4.6954E-5	1.1389E-5
7.1375E-6	-2.1082E-7

Figure S27. Derivation of Q_{st} for H_2 adsorption in PCN-46a from virial fitting of the total adsorption isotherm data. The virial coefficients are shown on the right.

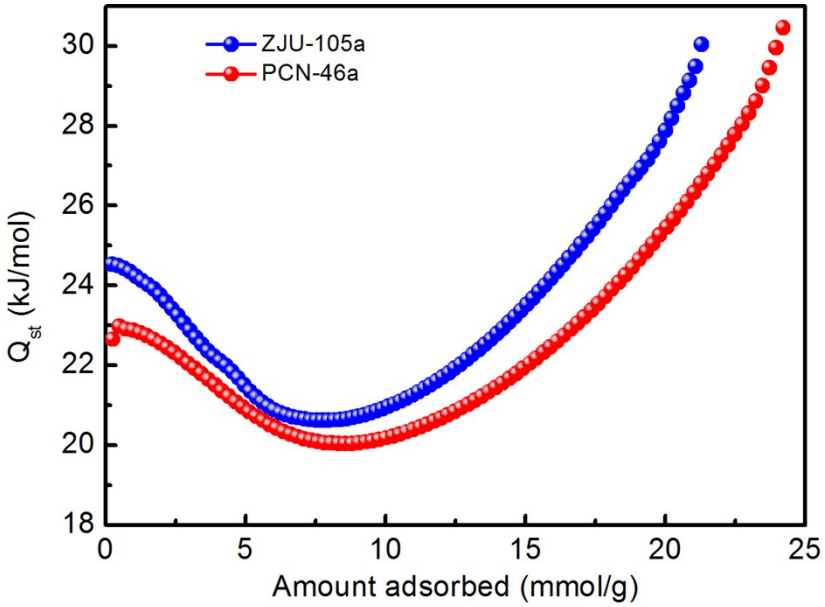

Figure S28. Comparison of Q_{st} for CO_2 adsorption for ZJU-105a and PCN-46a.

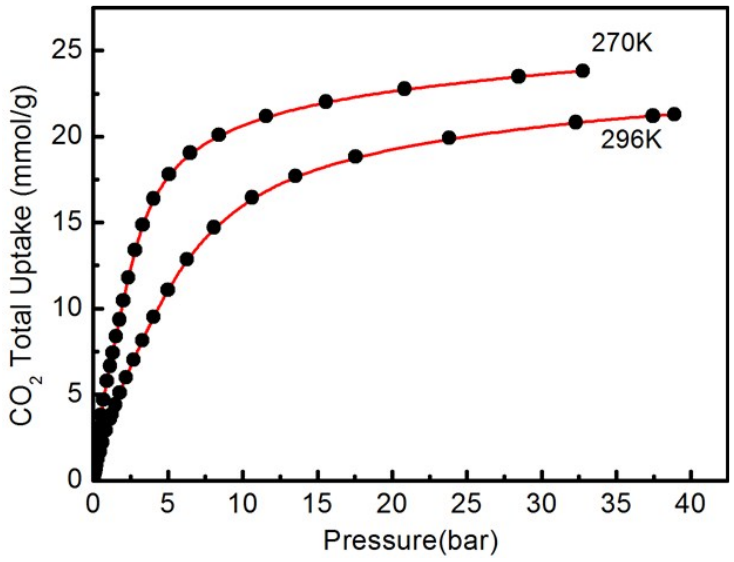

a_i	b_i
-2980.1	8.5918
69.056	-0.17122
3.9981	-0.0023269
-0.78485	0.0006758
0.01602	4.9051E-5
9.9883E-5	-1.8134E-6

Figure S29. Derivation of Q_{st} for CO_2 adsorption in ZJU-105a from virial fitting of the total adsorption isotherm data. The virial coefficients are shown on the right.

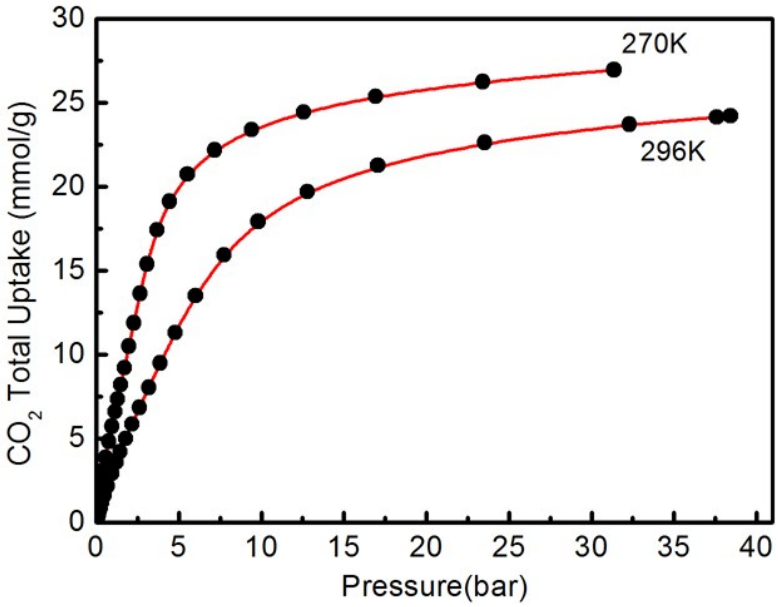

a_i	b_i
-2818.8	8.1877
79.364	-0.19781
-3.4214	0.010552
-0.085566	-3.0373E-7
0.0012768	1.02E-5
5.6299E-6	-4.3236E-8

Figure S30. Derivation of Q_{st} for CO_2 adsorption in PCN-46a from virial fitting of the total adsorption isotherm data. The virial coefficients are shown on the right.

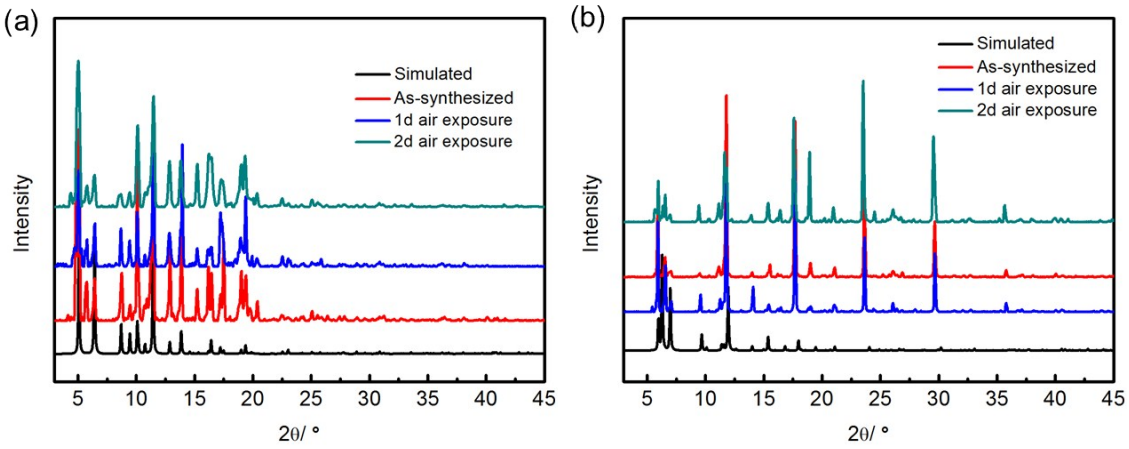

Figure S31. PXRD patterns of the as-synthesized ZJU-105 sample (a) andPCN-46 sample (b) after exposure to air for one or two days, respectively.

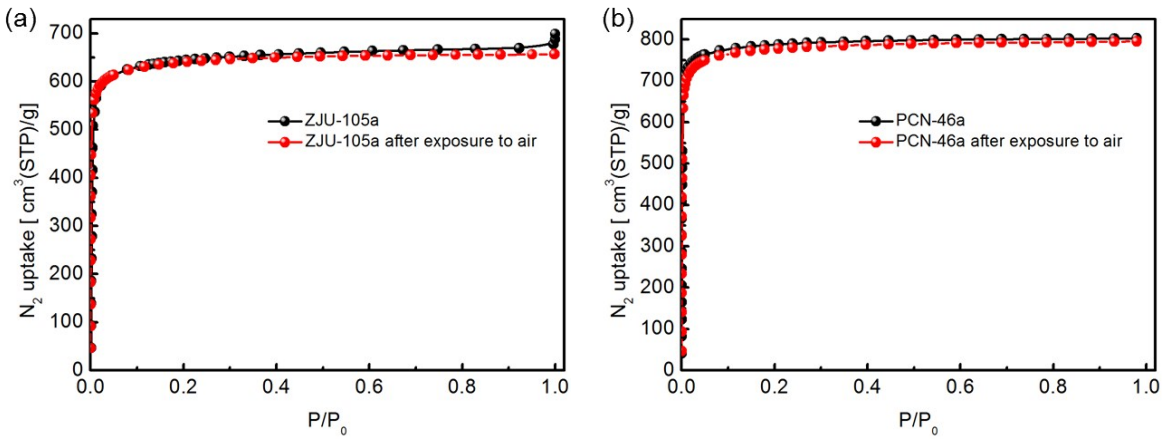

Figure S32. Comparison of N_2 adsorption isotherms of (a) ZJU-105a and (b) PCN-46a with the re-activated samples after exposure to air for two days, showing their relatively good air stability.

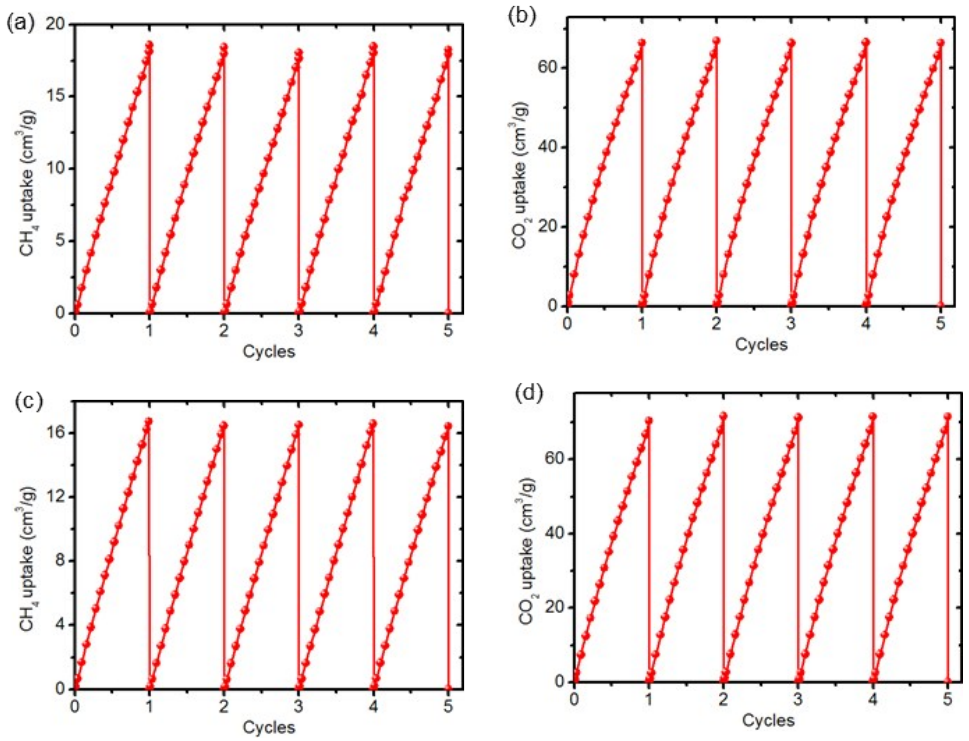

Figure S33. Cycles of CH_4 and CO_2 adsorption for ZJU-105a (a and b) and PCN-46a (c and d) at 298 K, indicating their good recyclability for gas storage.

Table S1. Crystallographic data and structure refinement results for ZJU-105 (from single-crystal X-ray diffraction analysis on the as-synthesized sample).

	ZJU-105
Formula	$C_{36}H_{18}Cu_2O_{10}$
Formula weight	737.58
Temperature/K	296(2)
Crystal system	Trigonal
Space group	R-3m
a, b (Å)	18.6721(4)
c (Å)	52.020(2)
α (°)	90
β (°)	90
γ (°)	120
V (Å^3)	15706.8(10)
Z	9
D_{calcd} (g cm^{-3})	0.702
μ (mm^{-1})	0.637
F(000)	3348
Crystal size/mm^3	0.32 × 0.28 × 0.24
GOF	1.059
R_{int}	0.0250
R_1, wR_2 [I>=2σ (I)]	0.0578, 0.1881
R_1, wR_2 [all data]	0.0725, 0.2080
Largest diff. peak and hole (e Å^{-3})	0.847 and -0.464
CCDC number	1943325

Table S2. Comparison of some promising MOFs for high-pressure CH_4 storage at 65/80 bar and 298 K.

MOFs	S_{BET}[a] (m^2/g)	V_p[b] (cm^3/g)	D_c[c] (g/cm^3)	total uptake at 65 bar cm^3/cm^3	Working capacity (5-65 bar) cm^3/cm^3	Total uptake at 80 bar cm^3/cm^3	Working capacity (5-80 bar) cm^3/cm^3	Q_{st} (kJ/mol)	Ref.
PCN-46a	**3224**	**1.243**	**0.619[d]**	**233**	**190**	**246**	**203**	**14.2**	**This work**
ZJU-105a	**2608**	**1.037**	**0.660**	**228**	**175**	**243**	**190**	**16.58**	**This work**
NOTT-102a	3342	1.268	0.587	233	185	-	-	14.90	3
MFM-115a	3394	1.38	0.611	238	191	256	208	16.3	4
MOF-905	3490	1.34	0.537	206	181	228	203	11.7	5
Al-soc-MOF-1	5585	2.3	0.34	197	176	221	201	11.0	6
HKUST-1	1850	0.78	0.883	267	190	272	200	17.0	7,12
MFM-112a	3800	1.62	0.503	218	181	236	200	16.2	4
NJU-Bai 43	3090	1.22	0.639	254	198	-	-	14.45	8
UTSA-110	3241	1.263	0.600	241	193	-	-	14.5	3
UTSA-76	2820	1.09	0.699	257	197	-	-	15.5	9
Co(BDP)	2911	1.02	0.774	203	197	203	197	13	10
MAF-38	2022	0.808	0.761	263	187	273	197	21.6	11
NJU-Bai 42	2830	1.07	0.693	247	193	-	-	14.49	8
Nu-125	3120	1.29	0.578	232	183	-	-	15.1	7
NU-111	4930	2.09	0.409	206	179	-	-	14.2	7
FDM-8	3643	1.54	0.563	193	171	215	193	10.4	13
MOF-905-Naph	3310	1.25	0.585	201	172	217	188	11.3	5
MOF-205	4460	2.16	0.38	185	166	205	186	10.6	14
MOF-177	4500	1.89	0.427	187	167	205	185	9.9	14
MOF-905-Me2	3640	1.39	0.568	213	186	211	184	10.3	5
PCN-14	2000	0.85	0.829	230	157	250	178	18.7	7,12
MOF-5	3800	1.55	0.590	203	181	198	176	10.0	7,12
Cu-tbo-MOF-5	3971	1.12	0.595	199	158	216	175	20.4	15
MOF-950	3440	1.30	0.517	195	160	209	174	11.9	5
MFM-132a	2466	1.06	0.650	201	150	213	162	15.7	4
X-dia-1-Ni	-	0.648	0.852	189	149	-	-	-	15
MOF-210	6240	3.6	0.25	141	128	166	153	-	5
Ni-MOF-74	1350	0.51	1.206	251	129	267	152	21.4	7,12

[a] BET surface areas calculated from N_2 isotherms at 77 K. [b] Pore volumes calculated from the maximum amounts of N_2 adsorbed. [c] Crystal densities without guest molecules and terminal water molecules. [d] Calculated from the crystal density of the activated PCN-46a originated from the literature 35.

Table S3. Comparison of some promising MOFs for high-pressure CH_4 storage at 100 bar and 298 K.

MOFs	S_{BET}[a] (m^2/g)	V_p[b] (cm^3/g)	D_c[c] (g/cm^3)	total uptake at 100 bar cm^3/cm^3	Working capacity (5-100 bar) cm^3/cm^3	Q_{st} (kJ/mol)	Ref.
PCN-46a	**3224**	**1.243**	**0.619**	**260**	**217**	**14.2**	**This work**
ZJU-105a	**2608**	**1.037**	**0.660**	**258**	**203**	**16.58**	**This work**
HKUST-1	1850	0.78	0.883	279	207	17.0	7,12
MOF-205	4460	2.16	0.38	220	201	10.6	5
MOF-177	4500	1.89	0.427	238	218	9.9	5
PCN-14	2000	0.85	0.829	263	191	18.7	7,12
MOF-5	3800	1.55	0.590	249	227	10.0	5
MOF-210	6240	3.6	0.25	202	189	-	5
Ni-MOF-74	1350	0.51	1.206	228	113	21.4	7,12

[a] BET surface areas calculated from N_2 isotherms at 77 K. [b] Pore volumes calculated from the maximum amounts of N_2 adsorbed. [c] Crystal densities without guest molecules and terminal water molecules.

Table S4. Comparison of H_2 Adsorption Data for a Variety of MOFs.

MOFs	S_{BET}[a] (m^2/g)	V_p[b] (cm^3/g)	D_c[c] (g/cm^3)	Total H_2 uptake				Ref.
				g/L	wt%	T (K)	P (bar)	
PCN-46a	**3224**	**1.243**	**0.619**	**50**	**7.47**	**77**	**65**	**This work**
ZJU-105a	**2608**	**1.037**	**0.660**	**48**	**6.78**	**77**	**65**	**This work**
NOTT-102a	3342	1.268	0.587	42	6.72	78	65	16
MOF-5	3320	1.38	0.610	50	7.58	77	65	17
NU-111	4930	2.09	0.409	49	10.71	77	65	18
MOF-177	4500	1.89	0.427	49	10.29	77	65	19
IRMOF-20	3409	1.53	0.511	48	8.59	77	65	17
NU-100	6143	2.82	0.273	47	14.68	77	65	20
NU-800	3149	1.34	0.554	44	7.36	77	65	21
NU-1100	4020	1.53	0.467	43	8.42	77	65	22
MOF-210	6240	3.6	0.250	41	14.09	77	65	23
MOF-200	4530	3.59	0.22	36	14.06	77	65	23
PCN-68	5109	2.13	0.380	35	8.43	77	65	24

[a] BET surface areas calculated from N_2 isotherms at 77 K. [b] Pore volumes calculated from the maximum amounts of N_2 adsorbed. [c] Crystal densities without guest molecules and terminal water molecules.

Table S5. Comparison of CO_2 Adsorption Data for a Variety of MOFs at RT.

MOFs	S_{BET}[a] (m^2/g)	V_p[b] (cm^3/g)	D_c[c] (g/cm^3)	Total uptake at 30 bar		Ref.
				g/g	cm^3/cm^3	
PCN-46a	**3224**	**1.243**	**0.619**	**1.04**	**328**	**This work**
ZJU-105a	**2608**	**1.037**	**0.660**	**0.91**	**309**	**This work**
NU-111	4930	2.09	0.409	1.68	350	18
PCN-11	1931	0.91	0.749	0.87	333	25
NiMOF-74	1218	0.47	1.206	0.54	332	26
NU-140	4300	1.97	0.426	1.52	330	27
NOTT-101	2805	1.08	0.684	0.95	328	16
ZJU-35a	2899	1.16	0.657	0.97	326	28
NU-125	3120	1.29	0.578	1.10	324	29
PCN-61	3000	1.36	0.560	1.11	318	24
MOF-177	4500	1.89	0.427	1.45	315	30
ZJU-5a	2823	1.07	0.679	0.91	313	31
MIL-101c	4230	2.15	0.440	1.39	313	32
ZJU-36a	4014	1.60	0.496	1.24	312	28
MOF-205	4460	2.16	0.380	1.61	312	23
UTSA-20	1655	0.63	0.910	0.67	312	33
Cu-TDPAT	1938	0.93	0.782	0.77	306	34
NU-100	6143	2.82	0.273	1.76	245	20
MOF-210	6240	3.6	0.250	1.70	216	23

[a] BET surface areas calculated from N_2 isotherms at 77 K. [b] Pore volumes calculated from the maximum amounts of N_2 adsorbed. [c] Crystal densities without guest molecules and terminal water molecules.

Disclaimer: Certain commercial equipment, instruments, or materials are identified in this paper to foster understanding. Such identification does not imply recommendation or endorsement by the National Institute of Standards and Technology, nor does it imply that the materials or equipment identified are necessarily the best available for the purpose.

Reference

1. W. Zhou, H. Wu, M. R. Hartman and T. Yildirim, *J. Phys. Chem. C*, 2007, **111**, 16131.
2. A. L. Spek, *J. Appl. Crystallogr.*, 2003, **36**, 7.
3. H.-M. Wen, B. Li, L. Li, R.-B. Lin, W. Zhou, G. Qian and B. Chen, *Adv. Mater.*, 2018, **30**, 1704792.
4. Y. Yan, D. I. Kolokolov, I. d. Silva, A. G Stepanov, A. J. Blake, A. Dailly, P. Manuel, C. C Tang, S. Yang and M. Schröder, *J. Am. Chem. Soc*., 2017, **139**, 13349.
5. J. Jiang, H. Furukawa, Y.-B. Zhang and O. M. Yaghi, *J. Am. Chem. Soc.*, 2016, **138**, 10244.
6. D. Alezi, Y. Belmabkhout, M. Suyetin, P. M. Bhatt, Ł. J. Weseliński, V. Solovyeva, K. Adil, I. Spanopoulos, P. N. Trikalitis, A.-H. Emwas and M. Eddaoudi, *J. Am. Chem. Soc*., 2015, **137**, 13308.
7. Y. Peng, V. Krungleviciute, I. Eryazici, J. T. Hupp, O. K. Farha and T. Yildirim, *J. Am. Chem. Soc*., 2013, **135**, 11887.
8. M. Zhang, W. Zhou, T. Pham, K. A. Forrest, W. Liu, Y. He, H. Wu, T. Yildirim, B. Chen, B. Space, Y. Pan, M. J. Zaworotko and J. Bai, *Angew. Chem., Int. Ed.*, 2017, **56**, 11426.
9. B. Li, H.-M. Wen, H. Wang, H. Wu, M. Tyagi, T. Yildirim, W. Zhou and B. Chen, *J. Am. Chem. Soc.,* 2014, **136**, 6207.
10. J. A. Mason, J. Oktawiec, M. K. Taylor, M. R. Hudson, J. Rodriguez, J. E. Bachman, M. I. Gonzalez, A. Cervellino, A. Guagliardi, C. M. Brown, P. L. Llewellyn, N. Masciocchi and J. R. Long, *Nature*, 2015, **527**, 357.
11. J.-M. Lin, C.-T. He, Y. Liu, P.-Q. Liao, D.-D. Zhou, J.-P. Zhang and X.-M. Chen, *Angew. Chem., Int. Ed.*, 2016, **55**, 4752.
12. J. A. Mason, M. Veenstra and J. R. Long, *Chem. Sci*., 2014, **5**, 32.
13. B. Tu, L. Diestel, Z.-L. Shi, W. R. L. N. Bandara, Y. Chen, W. Lin, Y.-B. Zhang, S. G. Telfer and Q. Li, *Angew. Chem., Int. Ed.*, 2019, **131**, 5402.
14. F. Gándara, H. Furukawa, S. Lee and O. M. Yaghi, *J. Am. Chem. Soc.*, 2014, **136**, 5271.
15. I. Spanopoulos, C. Tsangarakis, E. Klontzas, E. Tylianakis, G. Froudakis, K. Adil, Y. Belmabkhout, M. Eddaoudi and P. N. Trikalitis, *J. Am. Chem. Soc.*, 2016, **138**, 1568.
16. X. Lin, I. Telepeni, A. J. Blake, A. Dailly, C. M. Brown, J. M. Simmons, M. Zoppi, G. S. Walker, K. M. Thomas, T. J. Mays, P. Hubberstey, N. R. Champness and M. Schröder, *J. Am. Chem. Soc.*, 2009, **131**, 2159.
17. A. Ahmed, Y. Liu, J. Purewal, L. D. Tran, A. G. Wong-Foy, M. Veenstra, A. J. Matzger and D. J. Siegel, *Energy Environ. Sci.*, 2017, **10**, 2459.
18. Y. Peng, G. Srinivas, C. E. Wilmer, I. Eryazici, R. Q. Snurr, J. T. Hupp, T. Yildirim and O. K. Farha, *Chem. Commun.*, 2013, **49**, 2992.
19. H. Furukawa, M. A. Miller and O. M. Yaghi, *J. Mater. Chem*., 2007, **17**, 3197.
20. O. K. Farha, A. O. Yazaydin, I. Eryazici, C. D. Malliakas, B. G. Hauser, M. G. Kanatzidis, S. T. Nguyen, R. Q. Snurr and J. T. Hupp, *Nat. Chem*., 2010, **2**, 944.
21. D. A. Gomez-Gualdron, O. V. Gutov, V. Krungleviciute, B. Borah, J. E. Mondloch, J. T. Hupp, T. Yildirim, O. K. Farha and R. Q. Snurr , *Chem. Mater*., 2014, **26**, 5632.
22. O. V. Gutov, W. Bury, D. A. Gomez-Gualdron, V. Krungleviciute, D. Fairen-Jimenez, J. E. Mondloch, A. A. Sarjeant, S. S. Al-Juaid, R. Q. Snurr, J. T. Hupp, T. Yildirim and O. K. Farha, *Chem. – Eur. J.*, 2014, **20**, 12389.
23. H. Furukawa, N. Ko, Y. B. Go, N. Aratani, S. B. Choi, E. Choi, A. Ö. Yazaydin, R. Q. Snurr, M. O'Keeffe, J. Kim and O. M. Yaghi, *Science*, 2010, **329**, 424.
24. D. Yuan, D. Zhao, D. Sun and H.-C. Zhou, *Angew. Chem., Int. Ed*., 2010, **49**, 5357.

25. J. M. Simmons, H. Wu, W. Zhou and T. Yildirim, *Energy Environ. Sci*., 2011, **4**, 2177.
26. P. D. C. Dietzel, V. Besikiotis and R. Blom, *J. Mater. Chem*., 2009, **19**, 7362.
27. G. Barin, V. Krungleviciute, D. A. Gomez-Gualdron, A. A. Sarjeant, R. Q. Snurr, J. T. Hupp, T. Yildirim and O. K. Farha, *Chem. Mater.,* 2014, **26**, 1912.
28. G.-Q. Kong, Z.-D. Han, Y. He, S. Ou, W. Zhou, T. Yildirim, R. Krishna, C. Zou, B. Chen and C.-D. Wu, *Chem. – Eur. J.*, 2013, **19**, 14886.
29. C. E. Wilmer, O. K. Farha, T. Yildirim, I. Eryazici, V. Krungleviciute, A. A. Sarjeant, R. Q. Snurr and J. T. Hupp, *Energy Environ. Sci.*, 2013, **6**, 1158.
30. A. R. Millward and O. M. Yaghi, *J. Am. Chem. Soc*., 2005, **127**, 17998.
31. X. Rao, J. Cai, J. Yu, Y. He, C. Wu, W. Zhou, T. Yildirim, B. Chen and G. Qian, *Chem. Commun*., 2013, **49**, 6719.
32. P. L. Llewellyn, S. Bourrelly, C. Serre, A. Vimont, M. Daturi, L. Hamon, G. D. Weireld, J.-S. Chang, D.-Y. Hong, Y. K. Hwang, S. H. Jhung and G. Férey, *Langmuir*, 2008, **24**, 7245.
33. Z. Guo, H. Wu, G. Srinivas, Y. Zhou, S. Xiang, Z. Chen, Y. Yang, W. Zhou, M. O'Keeffe and B. Chen, *Angew. Chem., Int. Ed.*, 2011, **50**, 3178.
34. B. Li, Z. Zhang, Y. Li, K. Yao, Y. Zhu, Z. Deng, F. Yang, X. Zhou, G. Li, H. Wu, N. Nijem, Y. J. Chabal, Z. Lai, Y. Han, Z. Shi, S. Feng and J. Li, *Angew. Chem., Int. Ed*., 2011, **51**, 1412.
35. D. Zhao, D. Yuan, A. Yakovenko and H.-C. Zhou, *Chem. Commun.*, 2010, **46**, 4196.